The problem of energy conservation in one-way models

Michael B. Porter, Finn B. Jensen, and Carlo M. Ferla
SACLANT Undersea Research Centre, 19026 La Spezia, Italy

(Received 3 July 1990; accepted for publication 23 October 1990)

It is shown that the standard stair-step representation of a sloping bottom may result in significant prediction errors. In fact, current parabolic equation implementations are *not* energy conserving. The problem is shown to derive from the approximate treatment of the interface conditions at vertical boundaries along the stair steps. Several improved interface conditions are proposed.

PACS numbers: 43.30.Bp

INTRODUCTION

Since the early 1970's, when the first parabolic equation (PE) solution based on Fourier transforms appeared in the underwater acoustics community,[1] the PE technique has been applied extensively to model propagation in range-dependent ocean environments with strong bathymetric changes. In fact, the rationale behind the continual search for wider angle PE forms was to obtain an accurate treatment of bottom-interacting propagation, which often involves steep propagation angles. (Critical reflection angles of 20°–30° are typical for sandy seafloors.) Wide-angle PE's were subsequently used with confidence to model propagation in sloping bottom situations, both on continental shelves and over seamounts. There is, however, a fundamental problem of energy conservation in current PE implementations of sloping interfaces, a problem that was recognized just recently and which may result in prediction errors of several decibels for moderate bottom slopes.

Our discussion will focus on the cause and resolution of this problem in models that treat sloping bottoms by a staircase approximation. This type of approach is used in both parabolic equation and coupled-mode models, however, we should mention that there are some subtleties in using our results for finite-difference implementations of PE's. Energy conservation is intimately linked with the difference scheme used and should be verified for the discretized equations as well. We have performed a naive implementation of our interface conditions in a popular PE model (IFD)[2] and obtained improvements similar to those we shall present for the coupled-mode formulation, however, some problems of noise in the solution have simultaneously cropped up. Westwood and Collins[3] have performed more complete tests using a variable-angle PE and obtained satisfactory results.

Energy conservation for coupled-mode models that use a smooth bottom is discussed by Rutherford and Hawker.[4] An energy-conserving PE has also been formulated by Kriegsmann.[5] The "energy" conserved in the latter formulation does not precisely correspond to the energy that is conserved by the original Helmholtz equation, however, the model should provide an improvement. Lee and McDaniel[6] have constructed a modified bottom interface condition but it is unclear to what extent their formulation is energy conserving. Abrahamsson and Kreiss[7] specifically analyse energy conservation in the special case of a rigid bottom. Finally, it is possible to circumvent the staircase problem by simply picking a coordinate system parallel to the water/sediment interface as shown by Collins.[3] However, in the general case where there may be more than one sloping interface a simple grid rotation does not suffice.

We shall begin in Sec. I by reviewing the results of the ASA benchmark problem that motivated this work. In Sec. II, we study a simple one-dimensional wave equation to illustrate how these errors are induced by inaccurate treatment of the vertical interfaces. That analysis allows us to suggest improved interface conditions suitable for both PE and coupled-mode implementation. We have implemented the new interface conditions in a one-way coupled-mode formulation and in Secs. III and IV we demonstrate that they resolve the problem of energy conservation and as a result satisfy reciprocity to a high degree of accuracy. Finally, in Sec. V we end with a summary and conclusions.

I. ASA BENCHMARK RESULTS

Examples of inaccurate PE results for upslope propagation in wedge-shaped oceans first appeared among the range-dependent benchmark solutions solicited by the Acoustical Society of America in 1987.[8] A schematic of the environmental scenario is given in Fig. 1. The initial water depth is

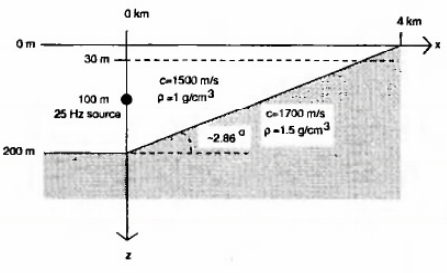

FIG. 1. Schematic of the wedge problem.

 0001-4966/91/031058-10$00.80

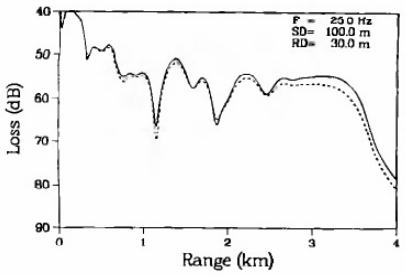

FIG. 2. Coupled-mode results for the 2.86° wedge [two way (—) and one way (- - -)].

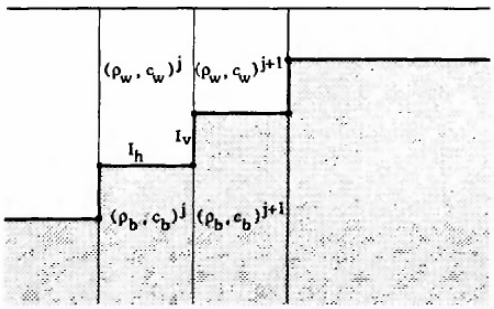

FIG. 4. Stair-step representation of sloping interface.

200 m decreasing linearly to 0 m at a range of 4 km giving a wedge angle of about 2.86°. The source frequency (F) is 25 Hz, while the source depth (SD) and receiver depth (RD) are, respectively, 100 and 30 m. The water sound speed is 1500 m/s, and the bottom speed is 1700 m/s. The density ratio between bottom and water is 1.5 and the bottom attenuation is 0.5 dB/λ.

The reference solution given by the solid line in Fig. 2 was obtained from a full-spectrum *two-way* coupled-mode solution.[9] On the same graph is displayed the one-way coupled-mode result that, as range increases, deviates increasingly from the reference solution. (At each interface, the one-way coupled-mode calculation matches pressure but not velocity. This approach is described in more detail in Sec. II.) In Fig. 3, we superimpose the one-way coupled-mode result with a solution obtained using a standard finite-difference parabolic equation model (IFD).[2] The PE solution, like most of the other PE results presented in the ASA benchmark session, agrees quite nicely with the *erroneous* one-way coupled-mode result.

This difference was initially thought to be due to the neglect of backscattering in the one-way solutions, but it was subsequently realized that the backscattered field in this case is negligible.[10] In fact, we find that the strength of the backscattered field component, extracted from the two-way coupled-mode result, is 40–50 dB lower than the outgoing field component.

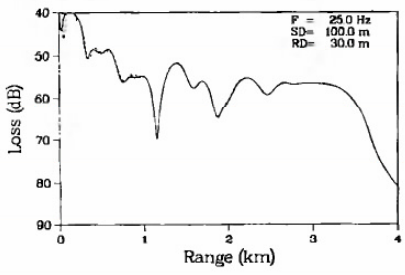

FIG. 3. One-way coupled mode (—) and PE results (- - -) for the 2.86° wedge.

Since the solution is essentially outgoing, then why are the one-way results in error? This can be easily understood by looking at the consequences of the use of a stair-step approximation to a sloping bottom. Figure 4 displays a few vertical segments separating media of different properties. The important interfaces with strong impedance contrasts are the horizontal interfaces I_h and the vertical interfaces I_v along the stair steps.

While conditions at horizontal interfaces (continuity of pressure and vertical particle velocity) are accurately implemented, the vertical interfaces I_v are treated very loosely. In fact, an *a priori* assumption of the solution being outgoing only permits just one vertical interface condition to be satisfied. When solving for pressure in a finite-difference PE implementation, the condition being satisfied is normally continuity of pressure across vertical interfaces. Since split-step Fourier implementations generally solve for a density-reduced pressure $p/\sqrt{\rho}$, these codes provide continuity of reduced pressure across vertical interfaces. It is clear, however, that the full-interface condition cannot in general be satisfied within the framework of a one-way solution.

II. TEST OF INTERFACE CONDITIONS: ONE-DIMENSIONAL WAVE EQUATION

We next address the question of which type of approximate interface condition should be used in one-way solutions in order to improve accuracy. Some guidance can be gained by examining a 1-D wave equation. Thus we consider a problem with $c(x)$ being the sound speed and $\rho(x)$ being the density as a function of axial distance x. The governing equation is then

$$\rho[(1/\rho)p_x]_x + [\omega^2/c^2(x)]p = 0, \tag{1}$$

where $p(x)$ is the acoustic pressure and ω is the frequency of the time-harmonic source.

We observe that for slowly varying $\rho(x)$, the WKB[11] approximation to $p(x)$ is given by

$$p(x) \sim A_0\sqrt{\{[\rho(x)/\rho_0][k_0/k(x)]\}}e^{i\int_0^x k(s)\,ds}, \tag{2}$$

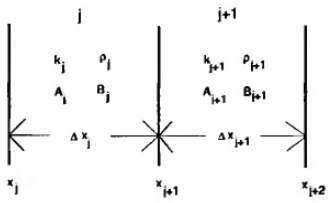

FIG. 5. Discretization of the 1-D wave equation.

where $k(x) = \omega/c(x)$. (The general form of the WKB representation involves terms corresponding to right and left traveling waves. We assume no reflected wave is generated so that the above form represents the complete solution.) Furthermore, it is easy to verify that the WKB result is energy conserving in the sense that $\mathrm{Im}(p^* p_x/\rho)$ is constant as a function of x.

We now consider the results obtained by a piecewise constant discretization. Thus, as illustrated schematically in Fig. 5, the medium is approximated by a sequence of N segments with both sound speed and density constant within a segment. The solution in the jth segment can then be written as the sum of a right- and left-traveling wave as follows:

$$p_j(x) = A_j e^{ik_j(x - x_j)} + B_j e^{-ik_j(x - x_j)}, \tag{3}$$

where x_j and x_{j+1} are the endpoints of the jth segment and k_j is the wave number in that segment. We next consider the effect of four possible interface conditions.

A. Pressure matching

In this case, we assume that $B_j = 0$ for each segment so that there is no backscattered field. Matching pressure at $x = x_{j+1}$, we obtain

$$A_{j+1} = A_j e^{ik_j \Delta x_j}, \tag{4}$$

which implies,

$$A_N = A_0 \prod_{j=0}^{N-1} e^{ik_j \Delta x_j} \tag{5}$$

$$= A_0 e^{i\sum_{j=0}^{N-1} k_j \Delta x_j}. \tag{6}$$

Now taking the limit as the number of segments goes to inifinty yields:

$$p(x) = A_0 e^{i\int_0^x k(s)\,ds}. \tag{7}$$

Notice that the phase term is identical to the WKB result of Eq. (2), however, the amplitude factor is wrong. The pressure-matched solution shows a constant amplitude, while the WKB amplitude varies in proportion $\sqrt{\rho(x)/k(x)}$.

B. Velocity matching

Again, we assume that $B_j = 0$ for each segment so that there is no backscattered field. Matching p_x/ρ at each interface we obtain

$$A_{j+1} = A_j [(\rho_{j+1}/\rho_j)(k_j/k_{j+1})] e^{ik_j \Delta x_j}, \tag{8}$$

which implies

$$A_N = A_0 \prod_{j=0}^{N-1} \frac{\rho_{j+1}}{\rho_j} \frac{k_j}{k_{j+1}} e^{ik_j \Delta x_j} \tag{9}$$

$$= A_0 [(\rho_N/\rho_0)(k_0/k_N)] e^{i\sum_{j=0}^{N-1} k_j \Delta x_j}. \tag{10}$$

Now taking the limit as the number of segments goes to infinity yields

$$p(x) = A_0 \{[\rho(x)/\rho_0][k_0/k(x)]\} e^{i\int_0^x k(s)\,ds}. \tag{11}$$

Once again, the phase factor is correct and the amplitude incorrect. The WKB amplitude term is the geometric mean of the pressure-matched and velocity-matched solutions.

C. Reduced-pressure matching

Matching $p/\sqrt{\rho}$ at each interface leads to

$$A_{j+1} = A_j \sqrt{(\rho_{j+1}/\rho_j)}\, e^{ik_j \Delta x_j}, \tag{12}$$

which implies,

$$A_N = A_0 \prod_{j=0}^{N-1} \sqrt{(\rho_{j+1}/\rho_j)}\, e^{ik_j \Delta x_j} \tag{13}$$

$$= A_0 \sqrt{(\rho_N/\rho_0)}\, e^{i\sum_{j=0}^{N-1} k_j \Delta x_j}. \tag{14}$$

Again, taking the limit as the number of segments goes to infinity yields

$$p(x) = A_0 \sqrt{(\rho(x)/\rho_0)}\, e^{i\int_0^x k(s)\,ds}. \tag{15}$$

Thus by matching reduced pressure we correct for the errors due to density variation but not for those due to the change in sound speed.

D. Impedance matching

It is evident that some additional correction is needed to account for the effect of variations in $k(x)$. We have experimented with various possibilities, however, we shall consider one in particular suggested by Westwood and Collins[3] and recently implemented in a PE code. In this approach, one simply matches $p/\sqrt{\rho c}$ across interfaces. (We refer to this as impedance matching although it actually involves the square root of the material impedance.) This implies

$$A_{j+1} = A_j \sqrt{[(\rho_{j+1}/\rho_j)(k_j/k_{j+1})]}\, e^{ik_j \Delta x_j}. \tag{16}$$

Following the now familiar sequence of steps one arrives at

$$p(x) = A_0 \sqrt{\{[\rho(x)/\rho_0][k_0/k(x)]\}}\, e^{i\int_0^x k(s)\,ds}, \tag{17}$$

which agrees precisely with the energy conserving WKB result.

For one-dimensional problems, this corrects for sound-speed changes as well as density changes across interfaces. However, for two-dimensions some complications arise. The difficulties are somewhat clearer if we consider an alternate derivation. Consider an energy flux defined by

$$E(x) = \int \mathrm{Im}\left(\frac{p^* p_x}{\rho}\right) dz. \tag{18}$$

The problem is to produce a matching condition that con-

serves this quantity. If we make the following plane-wave approximation,

$$p_x \approx ik_0 p, \tag{19}$$

with k_0 range independent, we obtain

$$E(x) \approx k_0 \int \frac{|p|^2}{\rho}\, dz. \tag{20}$$

In this plane-wave approximation $p/\sqrt{\rho}$ matching is a sufficient condition for energy conservation.

In general, we might expect to do better by correcting for variations in the average wave number with range. This leads to an improved approximation,

$$p_x \approx ik_0(x,z)p, \tag{21}$$

with

$$k_0(x,z) = \omega/c(x,z). \tag{22}$$

We then obtain,

$$E(x) \approx \int \frac{k_0(x,z)|p|^2}{\rho}\, dz. \tag{23}$$

From this equation we can see that, in this improved plane-wave approximation, a sufficient condition for conserving $E(x)$ is that $p/\sqrt{\rho c}$ is continuous. However, in general the pressure field involves a spread of plane-wave angles so that even the improved plane-wave approximation is in error. For this reason, matching $p/\sqrt{\rho c}$ does not entirely resolve the energy conservation problem in two dimension. However, in one dimension, there is a unique $k_0(x)$ that characterizes the wave so that the approximation becomes an equality and energy is conserved.

E. Single scatter

The single-scatter result is obtained by treating each pair of segments as an independent problem, thus neglecting the higher-order terms resulting from multiple scattering (reflection and transmission) at other interfaces. For problems involving simply sound-speed variation (not density variation) Bremmer[12] has shown that the single-scatter solution converges to the WKB result in the limit of an infinitely fine segmentation. However, the impedance contrast in our problem is dominated by the density change at interfaces and so we must reconsider the question of whether an energy conserving WKB solution is recovered.

In the left segment, we allow both an incident right-traveling wave with coefficient A_j and a reflected left-traveling wave with coefficinet B_j. In the right segment, we allow only an outgoing transmitted wave with coefficient A_{j+1}. The two unknowns permit us to impose both continuity of pressure and particle velocity:

$$A_{j+1} = A_j e^{ik_j \Delta x_j} + B_j e^{-ik_j \Delta x_j}, \tag{24}$$

$$A_{j+1} = (\rho_{j+1}/\rho_j)(k_j/k_{j+1}) \times \left(A_j e^{ik_j \Delta x_j} - B_j e^{-ik_j \Delta x_j}\right). \tag{25}$$

Solving for A_{j+1}, we obtain

$$A_{j+1} = A_j\{2e^{ik_j \Delta x_j}/[1 + (\rho_j/\rho_{j+1})(k_{j+1}/k_j)]\}, \tag{26}$$

which implies,

$$A_N = A_0 \prod_{j=0}^{N-1} \frac{2e^{ik_j \Delta x_j}}{1 + (\rho_j/\rho_{j+1})(k_{j+1}/k_j)} \tag{27}$$

$$= A_0 \prod_{j=0}^{N-1} \frac{2}{1 + f_{j+1}/f_j} e^{i\sum_{j=0}^{N-1} k_j \Delta x_j}, \tag{28}$$

where $f_j = k_j/\rho_j$.

Let us focus our attention on the term Q defined by,

$$Q = \lim_{N\to\infty} \prod_{j=0}^{N-1} \frac{2}{1 + f_{j+1}/f_j}. \tag{29}$$

Following Bremmer, we rewrite this as

$$Q = \lim_{N\to\infty} \exp\left(\sum_{j=0}^{N-1} \ln \frac{2}{1 + f_{j+1}/f_j}\right) \tag{30}$$

$$= \lim_{N\to\infty} \exp\left[-\sum_{j=0}^{N-1} \ln\left(1 + \frac{\Delta f_j}{2f_j}\right)\right] \tag{31}$$

where, $\Delta f_j = f_{j+1} - f_j$. Now, taking the limit and using the small x approximation $\ln(1+x) \approx x$ we obtain:

$$Q = \exp\left(-\int_{x_0}^{x} \frac{df}{2f}\right) = \exp\left(-\frac{1}{2} \ln \frac{f(x)}{f(x_0)}\right) \tag{32}$$

$$= \sqrt{\frac{f(x_0)}{f(x)}}. \tag{33}$$

Substituting this result back in Eq. (28) yields

$$p(x) = A_0 \sqrt{\frac{\rho(x)}{\rho_0} \frac{k_0}{k(x)}}\, e^{i\int_0^x k(s)\,ds}, \tag{34}$$

which is precisely the WKB result. The WKB result is of course only an approximation itself to the exact solution. Further improvements could be obtained by including additional terms in the multiple-scattering series as discussed by Bremmer.

F. Summary of results

The results of these various interface conditions are summarized as follows:

$e^{i\int_0^x k(s)\,ds}$	
$\frac{\rho(x)}{\rho_0} \frac{k_0}{k(x)} e^{i\int_0^x k(s)\,ds}$	p matched
$\sqrt{\frac{\rho(x)}{\rho_0}}\, e^{i\int_0^x k(s)\,ds}$	p_x/ρ matched
$\sqrt{\frac{\rho(x)}{\rho_0} \frac{k_0}{k(x)}}\, e^{i\int_0^x k(s)\,ds}$	$p/\sqrt{\rho}$ matched $p/\sqrt{\rho c}$ matched/single scatter/WKB

Comparing these forms we see that the pressure-matched solution shows serious deficiencies for moderate density variation. Velocity matching is also a poor choice, however, reduced-pressure matching corrects entirely for the density effect. If $c(x)$ varies much less than $\rho(x)$ the reduced-pressure matching would correct most of the error. A further improvement may be obtained using the single-scatter approximation.

The above discussion assumes a problem involving *continuous* variation of the material properties. For problems where discontinuities are present then both pressure matching and reduced-pressure matching may well provide inaccurate solutions. Consider for instance a simple interface between media with the same sound speed but with a density contrast. In the exact solution, an incident wave would partition its energy between a backscattered and forward traveling component. The reduced-pressure matching condition provides perfect energy conservation and therefore *erroneously* carries all the incident energy into the forward traveling component. In this case, only the single-scatter solution would provide the correct partitioning of energy. The single-scatter approximation in turn breaks down when significant energy results from multiple scattering involving additional interfaces.

The above interface conditions are all amenable to implementation in 2-D or 3-D wave equations involving either coupled mode or parabolic equation types of models. In the next section, we show the results of implementing these different interface conditions in a full-spectrum coupled-mode model.[9] The actual implementation details are fairly straightforward and are relegated to the appendix.

III. COUPLED-MODE RESULTS

A. Upslope propagation

Since the problem of energy conservation in PE's tends to be accentuated by increasing the bottom slope, we have here selected a somewhat extreme situation where the wedge-shaped ocean has a slope angle of 12.7°. As indicated schematically in Fig. 6, the initial water depth is 1000 m decreasing linearly to 100 m at a range of 4 km. The source, which is treated as a line source in plane geometry, is located at a depth of 50 m and has a frequency of 25 Hz. The water sound speed is 1500 m/s while the bottom speed is 1700 m/s.

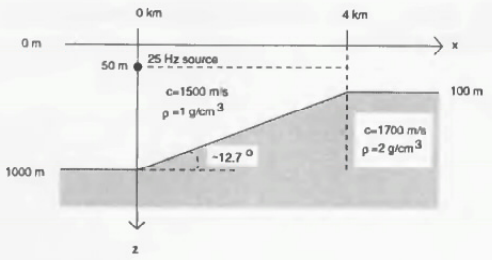

FIG. 6. Schematic of the modified wedge problem (upslope).

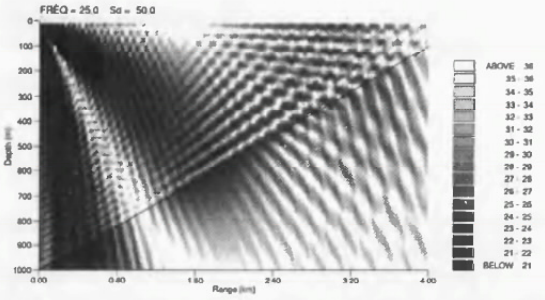

FIG. 7. Transmission loss for the modified wedge problem (upslope).

The density ratio between bottom and water is 2.0 and the bottom attenuation is 0.5 dB/λ.

In Fig. 7, we display our reference solution obtained from a full two-way calculation and in Fig. 8 we have extracted a horizontal slice taken at a receiver depth of 50 m. As in the original benchmark problem,[8] the pressure-matched solution is in error. With the increased slope and density contrast the solution now shows an even larger error of about 7 dB at 4 km.

The plot of the backscattered field in Fig. 9 shows that the backscatter is now significantly stronger than in the 2.86° wedge. Nevertheless, throughout most of the range, the backscattered field is negligible relative to the outgoing component.

In Fig. 10, we compare the full two way, the outgoing component, and the single-scatter solutions over the region from 3–4 km. The full two way and the outgoing component agree to within roughly 1 dB. This represents the difference due to the effect of backscattering. However, the key point of interest is that the improved one-way formulation based on the single-scatter approximation eliminates almost entirely the 7-dB error we have seen in the conventional pressure-matched solution. This approach is the most accurate in the hierarchy of one-way algorithms we have considered.

The single-scatter approach provides a nearly complete

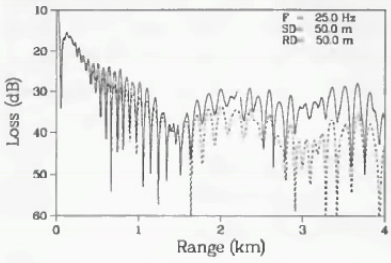

FIG. 8. Coupled-mode results for the 12.7° wedge [two way (—) and pressure matched (- - -)].

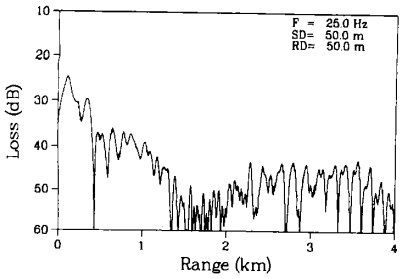

FIG. 9. Backscattered component of the two-way coupled-mode results for the 12.7° wedge.

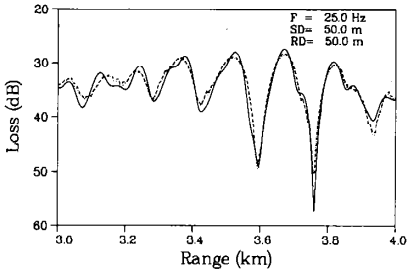

FIG. 10. Coupled-mode results for the 12.7° wedge [two way (—), outgoing component (- - -), and single scatter (···)].

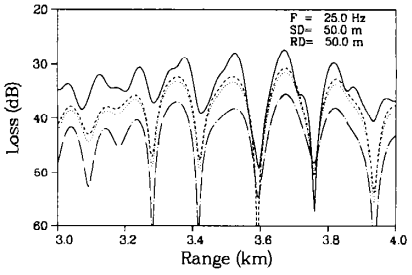

FIG. 11. Coupled-mode results for the 12.7° wedge [two way (—), $p/(\rho c)^{1/2}$ matched (- - -), $p/\rho^{1/2}$ matched (···), and p matched (-·-·)].

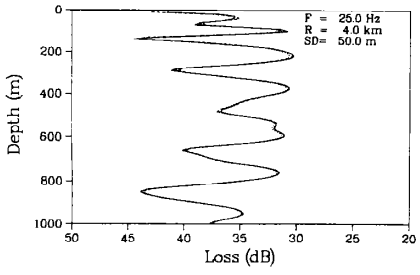

FIG. 12. Coupled-mode results for the 12.7° wedge [two way (—), outgoing component (- - -), and single-scatter (···)].

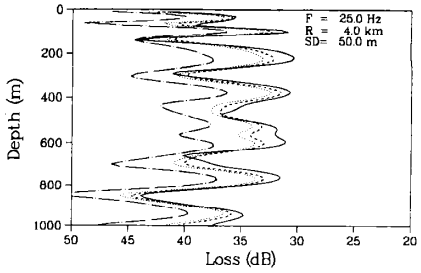

FIG. 13. Coupled-mode results for the 12.7° wedge [two way (—), $p/(\rho c)^{1/2}$ matched (- - -), $p/\rho^{1/2}$ matched (···), and p matched (-·-·)].

resolution of the problem of energy conservation. It is however somewhat more cumbersome than the other matching conditions. As shown in Fig. 11, reduced-pressure matching also provides a significant reduction in error compared to the simple pressure-matched solution.

As discussed in the previous section, matching $p/\sqrt{\rho c}$ across interfaces resolves the energy conservation problem in one dimension but not necessarily in two dimension. However, we see in Fig. 11 this condition does provide a further improvement over reduced-pressure matching.

In Figs. 12 and 13, we consider the effects of these various interface conditions on transmission loss versus *depth* taken at a range of 4 km. At this particular range, the backscattered component is negligible so that the outgoing component and the full two-way solution (Fig. 12) agree almost perfectly. Again, we see that the single-scatter result provides nearly perfect agreement with the exact solution. Similarly, the improvements obtained by matching $p/\sqrt{\rho}$ (reduced pressure) or $p/\sqrt{\rho c}$ are seen in Fig. 13 to be fairly consistent over depth.

B. Downslope propagation

We now consider the case of downslope propagation as indicated schematically in Fig. 14. The initial water depth is now 100 m increasing linearly to 1000 m at a range of 4 km. The remaining properties are unchanged.

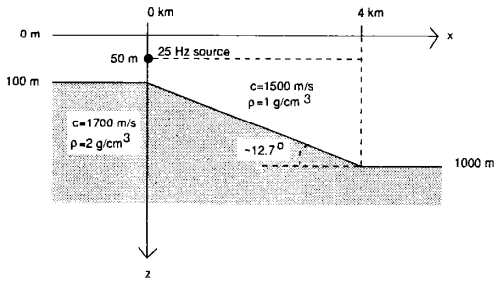

FIG. 14. Schematic of the modified wedge problem (downslope).

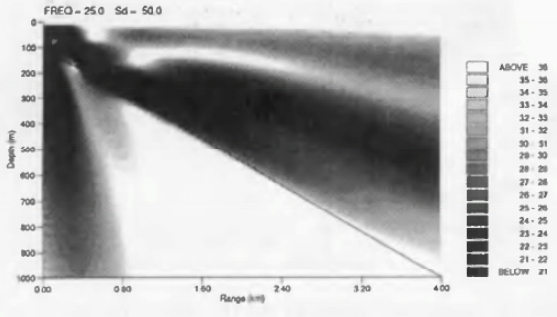

FIG. 15. Transmission loss for the modified wedge problem (downslope).

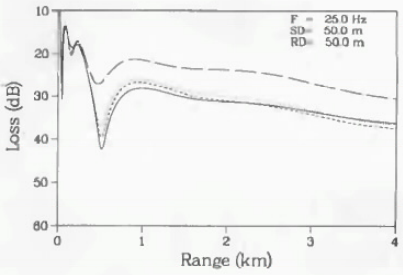

FIG. 17. Coupled-mode results for the 12.7° wedge [two way (—), $p/(\rho c)^{1/2}$ matched (- - -), $p/\rho^{1/2}$ matched (···), and p matched (-·-·-)].

In Fig. 15, we display our reference solution obtained from a full two-way calculation. In the downslope direction, there is less backscatter so that the two-way solution and the outgoing component of the two-way solution shown in Fig. 16 are almost identical along the entire receiver track. The single-scatter result once again provides a nearly exact treatment of the problem in a one-way context.

As shown in Fig. 17, the conventional pressure matching again produces an error of about 7 dB at a range of 4 km. However, this time the pressure-matched solution predicts too high an energy level. Matching reduced-pressure again eliminates most of the error while $p/\sqrt{\rho c}$ matching provides an improvement at some ranges and a degradation at other ranges.

Figures 18 and 19 show analogous results taken along a depth slice at a range of 4 km. Throughout the upper 1000 m the full two way, the outgoing component of the two-way solution and the single-scatter solution agree to within the accuracy of the calculations (Fig. 18). Reduced-pressure matching provides an alternative approach to eliminating the error as shown in Fig. 19. However, at this range $p/\sqrt{\rho c}$ matching produces an over correction.

To summarize the results of the upslope and downslope calculations, the reduced-pressure matching as implemented in most *split-step* PE's, produces a consistent improvement. As we have seen in the 1-D analysis reduced-pressure matching corrects only for the density effect and not the wave-number change. Nevertheless, considering that this test problem represents an extreme case, we may conclude that the $p/\sqrt{\rho}$ matching is adequate for most practical problems in underwater acoustics. However, the pressure matching currently implemented in finite-difference PE's is definitely not adequate.

The most accurate solution is based on the single-scatter formulation. This type of matching condition also lends itself to a simple marching solution and like the other approximations considered here is adaptable to other one-way models such as those based on parabolic equations. It is, however, somewhat more complicated than the other approximations. A simpler approximate single-scatter solution is formulated in Appendix A and provides answers that are almost identical to the single-scatter result.

Note that the standard pressure matching inherent in most finite-difference and finite-element PE's results in level errors of 5–7 dB, with energy loss for upslope propagation and energy gain for downslope propagation. Thinking of the up- and downslope cases as representing propagation into regions of higher and lower mean density, we can say that

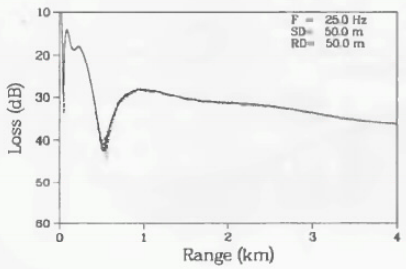

FIG. 16. Coupled-mode results for the 12.7° wedge [two way (—), outgoing component (- - -), and single scatter (···)].

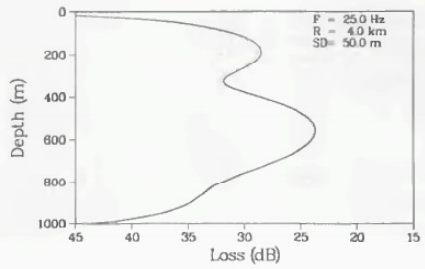

FIG. 18. Coupled-mode results for the 12.7° wedge [two way (—), outgoing component (- - -), and single scatter (···)].

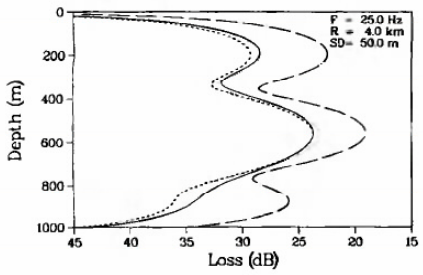

FIG. 19. Coupled-mode results for the 12.7° wedge [two way (—), $p/(\rho c)^{1/2}$ matched (- - -), $p/\rho^{1/2}$ matched (···), and p matched (-·-·-)].

the energy loss and gain in the two cases is consistent with the errors predicted by the 1-D analysis in the previous section. The magnitude of the error varies in a complicated manner with the parameters of the problem, but in our tests with the wedge problem tends to increase with density contrast and slope.

IV. RECIPROCITY

A simple but often neglected check on solution accuracy can be done by interchanging source and receiver and verifying that the transmission loss is identical at the receiver. According to the *principle of reciprocity*, this property should hold for problems with arbitrary sound-speed dependence even when absorption is present. (This is discussed more completely in Ref. 13.) Of course, this is a necessary but not sufficient condition for solution accuracy since even an incorrect model may happen to satisfy reciprocity. Nevertheless, this simple test is useful in eliminating many incorrect solutions.

In Fig. 20, we present transmission loss curves taken with source and receiver at a depth of 50 m in the wedge. (Other properties of the wedge problem are unchanged.) The solutions obtained using the traditional pressure-matching condition show a discrepancy of more than 12 dB between the upslope and downslope solutions (dashed lines): Even if we did not know the exact solution, we could conclude that at least one of the solutions is in serious error. In contrast, the single-scatter solution satisfies reciprocity to within 0.2 dB as indicated by the coincidence of the upslope and downslope curves (solid lines) at a range of 4 km.

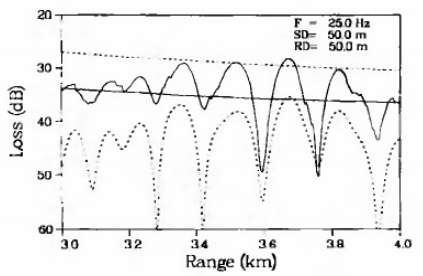

FIG. 20. Reciprocal propagation results. Superposition of upslope and downslope results using the single-scatter formulation (—), and pressure matching (- - -).

V. SUMMARY AND CONCLUSIONS

We have shown that certain common one-way formulations used in both PE and coupled-mode models treat vertical interfaces in an approximate fashion leading to energy loss for upslope propagation and energy gain for downslope propagation. Improved interface conditions have been suggested based on an analysis of the simpler 1-D wave equation and validated using a one-way coupled-mode formulation. Similarly modified interface conditions have recently been implemented in a finite-element PE demonstrating the anticipated improvements for PE models as well.[3]

ACKNOWLEDGMENTS

We have benefited from general discussions with Richard Evans in the course of this work. In particular, the suggestion of the single-scatter approach and the two-way coupled-mode code were provided by him.

APPENDIX A: COUPLED-MODE FORMULATION FOR THE SINGLE-SCATTER APPROXIMATION

Let us first review the basic coupled-mode formulation following closely Evans.[9] As for the 1-D wave equation, we begin by dividing the problem into N segments in range. Neglecting contributions from higher-order modes, the general solution in the jth segment can be written as follows:

$$p^j(r,z) = \sum_{m=1}^{M} [a^j_m \hat{H}1^j_m(r) + b^j_m \hat{H}2^j_m(r)] Z^j_m(z), \tag{A1}$$

where $\hat{H}1$, 2 are the following ratios of Hankel functions:

$$\hat{H}1^j_m(r) = [H_0^{(1)}(k^j_m r)/H_0^{(1)}(k^j_m r_{j-1})], \tag{A2}$$

$$\hat{H}2^j_m(r) = [H_0^{(2)}(k^j_m r)/H_0^{(2)}(k^j_m r_{j-1})], \tag{A3}$$

and $Z_m(z)$ is the mth mode of the depth-separated equation:

$$\rho(z)\frac{d}{dz}\left(\frac{1}{\rho(z)}\frac{dZ(z)}{dz}\right) + \left(\frac{\omega^2}{c^2(z)} - k^2\right) Z(z) = 0,$$

$$Z(0) = 0,$$

$$\frac{dZ}{dz}(D) = 0. \tag{A4}$$

In the remainder of this analysis, we replace the Hankel functions by their large argument asymptotic representation:

$$\hat{H}1^j_m(r) \sim H1^j_m(r) = \sqrt{(r_{j-1}/r)}\, e^{ik^j_m(r-r_{j-1})}, \tag{A5}$$

$$\hat{H}2^j_m(r) \sim H2^j_m(r) = \sqrt{(r_{j-1}/r)}\, e^{-ik^j_m(r-r_{j-1})}. \tag{A6}$$

Next, we impose continuity of pressure at the jth interface that leads to

$$\sum_{m=1}^{M} (a_m^{j+1} + b_m^{j+1}) Z_m^{j+1}(z)$$

$$= \sum_{m=1}^{M} [a_m^j H1_m^j(r_j) + b_m^j H2_m^j(r_j)] Z_m^j(z). \quad \text{(A7)}$$

This matching condition involves a continuum of depth points in that we require continuity of pressure for all z values. In practice, however, we are going to work with a limited mode set and therefore we need a finite set of conditions that relate the M mode coefficients a_m, b_m. This can be done in several ways. For instance, we could require continuity of pressure at M discrete depth points z_m, $m = 1,...,M$. We shall impose a moment condition that the error considered as a function of depth should have vanishing components of each of the first M modes. Thus we apply the operator,

$$\int \frac{(\cdot) Z_l^{j+1}(z)}{\rho_{j+1}(z)}\, dz, \quad \text{(A8)}$$

to our matching equation where $l = 1,...,M$. Because of the orthogonality property,

$$\int \frac{Z_m^{j+1}(z) Z_l^{j+1}(z)}{\rho_{j+1}(z)}\, dz = \delta_{lm}, \quad \text{(A9)}$$

only one term remains from the sum on the left. Therefore, we have

$$a_l^{j+1} + b_l^{j+1} = \sum_{m=1}^{M} [a_m^j H1_m^j(r_j) + b_m^j H2_m^j(r_j)] \tilde{c}_{lm}, \quad \text{(A10)}$$

where

$$\tilde{c}_{lm} = \int \frac{Z_l^{j+1}(z) Z_m^j(z)}{\rho_{j+1}(z)}\, dz. \quad \text{(A11)}$$

In matrix notation, we can write this equation as

$$\mathbf{a}^{j+1} + \mathbf{b}^{j+1} = \tilde{\mathbf{C}}^j (\mathbf{H}_1^j \mathbf{a}^j + \mathbf{H}_2^j \mathbf{b}^j), \quad \text{(A12)}$$

where, $\mathbf{H}_1^j$ and $\mathbf{H}_2^j$ denote the diagonal matrices with entries $H1_m^j(r_j)$ and $H2_m^j(r_j)$, respectively. In addition, $\tilde{\mathbf{C}}$ is the matrix with entries $\tilde{c}_{lm}$ and $\mathbf{a}$, $\mathbf{b}$ are column vectors with entries a_l, b_l, respectively.

We next impose continuity of radial particle velocity. The particle velocity is proportional to

$$\frac{1}{\rho_j} \frac{\partial p^j(r,z)}{\partial r}$$

$$\approx \frac{1}{\rho_j} \sum_{m=1}^{M} k_m^j [a_m^j H1_m^j(r) - b_m^j H2_m^j(r)] Z_m^j(z). \quad \text{(A13)}$$

This time we apply the operator,

$$\int (\cdot) Z_l^{j+1}(z)\, dz, \quad \text{(A14)}$$

to obtain

$$(a_l^{j+1} - b_l^{j+1}) = \sum_{m=1}^{M} [a_m^j H1_m^j(r_j) + b_m^j H2_m^j(r_j)] \hat{c}_{lm}, \quad \text{(A15)}$$

where

$$\hat{c}_{lm} = \frac{k_m^j}{k_l^{j+1}} \int \frac{Z_l^{j+1}(z) Z_m^j(z)}{\rho_j(z)}\, dz. \quad \text{(A16)}$$

Note that $\hat{c}_{lm}$ differs from $\tilde{c}_{lm}$ in the density term of the integral and by a ratio of horizontal wave numbers.

In matrix notation, this matching condition can be written as

$$\mathbf{a}^{j+1} - \mathbf{b}^{j+1} = \hat{\mathbf{C}}^j (\mathbf{H}_1^j \mathbf{a}^j + \mathbf{H}_2^j \mathbf{b}^j). \quad \text{(A17)}$$

Combining this equation with the pressure-matching condition of Eq. (A12), we obtain an explicit expression for $\mathbf{a}^{j+1}$ and $\mathbf{b}^{j+1}$:

$$\begin{bmatrix} \mathbf{a}^{j+1} \\ \mathbf{b}^{j+1} \end{bmatrix} = \begin{bmatrix} \mathbf{R}_1 & \mathbf{R}_2 \\ \mathbf{R}_3 & \mathbf{R}_4 \end{bmatrix} \begin{bmatrix} \mathbf{a}^j \\ \mathbf{b}^j \end{bmatrix}, \quad \text{(A18)}$$

where

$$\mathbf{R}_1^j = \tfrac{1}{2}(\tilde{\mathbf{C}}^j + \hat{\mathbf{C}}^j)\mathbf{H}_1^j, \quad \mathbf{R}_2^j = \tfrac{1}{2}(\tilde{\mathbf{C}}^j - \hat{\mathbf{C}}^j)\mathbf{H}_2^j,$$
$$\mathbf{R}_3^j = \tfrac{1}{2}(\tilde{\mathbf{C}}^j - \hat{\mathbf{C}}^j)\mathbf{H}_1^j, \quad \mathbf{R}_4^j = \tfrac{1}{2}(\tilde{\mathbf{C}}^j + \hat{\mathbf{C}}^j)\mathbf{H}_2^j. \quad \text{(A19)}$$

In the two-way coupled-mode approach, these local matching conditions would be assembled into a global matrix with one block for each interface. For the single-scatter approximation, the incoming wave in the left segment is assumed given and we require that the solution is purely outgoing in the right segment, i.e., $\mathbf{b}^{j+1} = \mathbf{0}$. Solving for the backscattered amplitudes, $\mathbf{b}^j$, we find:

$$\mathbf{b}^j = -\mathbf{R}_4^{-1} \mathbf{R}_3 \mathbf{a}^j. \quad \text{(A20)}$$

Therefore, the forward-scattered amplitudes, $\mathbf{a}^{j+1}$, are given by

$$\mathbf{a}^{j+1} = (\mathbf{R}_1 - \mathbf{R}_2 \mathbf{R}_4^{-1} \mathbf{R}_3) \mathbf{a}^j, \quad \text{(A21)}$$

which is an explicit equation for the forward-scattered field. The field in any given segment can then be computed by summing the terms in the modal sum representing the forward-scattered field.

We find from computational tests that an *approximate single-scatter* solution works nearly as well. This solution is obtained by neglecting lower-order terms in the single-scatter recursion:

$$\mathbf{a}^{j+1} = \mathbf{R}_1 \mathbf{a}^j. \quad \text{(A22)}$$

Note that the matrix $\mathbf{R}_1$ is an arithmetic mean of coupling matrices based on pressure matching and velocity matching. In other words, the solution is obtained by separately matching pressure and matching velocity at each interface and then averaging the resulting pressure fields before continuing the forward march. Like the single-scatter solution, one can show that the approximate single-scatter solution converges to the WKB form in the limit of an infinite number of segments.

The approximate single-scatter solution has the advantage that it can be computed without explicitly computing the coupling matrix $\mathbf{R}_1$. Details are provided below for the slightly simpler case of reduced-pressure matching.

APPENDIX B: COUPLED-MODE FORMULATION FOR THE REDUCED-PRESSURE MATCHING APPROXIMATION

Neglecting backscatter, the reduced pressure in the jth segment is given by,

$$\frac{1}{\sqrt{\rho_j}} p^j(r,z) \sim \frac{1}{\sqrt{\rho_j}} \sum_{m=1}^{M} a_m^j H_1^j{}_m(r) Z_m^j(z). \tag{B1}$$

The condition of continuity at each interface can therefore be written,

$$\frac{1}{\sqrt{\rho_{j+1}}} \sum_{m=1}^{M} a_m^{j+1} Z_m^{j+1}(z) = \frac{1}{\sqrt{\rho_j}} \sum_{m=1}^{M} a_m^j H_1^j{}_m(r_j) Z_m^j(z). \tag{B2}$$

In order to take advantage of the mode orthogonality, we apply the operator,

$$\int (\cdot) \frac{Z_l^{j+1}(z)}{\sqrt{\rho_{j+1}(z)}} dz, \tag{B3}$$

yielding

$$a_l^{j+1} = \sum_{m=1}^{M} a_m^j H_1^j{}_m(r_j) \bar{c}_{lm}, \quad l = 1,...,M, \tag{B4}$$

where

$$\bar{c}_{lm} = \int \frac{Z_l^{j+1}(z) Z_m^j(z)}{\sqrt{\rho_j(z)\rho_{j+1}(z)}} dz. \tag{B5}$$

The denominator in this coupling term is a geometric mean of the analogous terms obtained using pressure matching and velocity matching.

In matrix form, Eq. (B4) can be written,

$$\mathbf{a}^{j+1} = \bar{\mathbf{C}} \mathbf{H}_1^j \mathbf{a}^j. \tag{B6}$$

We shall perform one final manipulation of this result. Let us assume that the modes are finely tabulated on some grid of depth points. The mth vector is then used to define the mth column of a matrix $\mathbf{U}^j$. For an isodensity problem, we can then approximate the coupling matrix by the discrete form,

$$\bar{\mathbf{C}}^j \approx (\mathbf{U}^{j+1})^t \mathbf{U}^j, \tag{B7}$$

which is equivalent to evaluating the coupling integral by the trapezoidal rule. (For a variable density problem, this equation is slightly modified.) Substituting in Eq. (B6), we obtain

$$\mathbf{a}^{j+1} \approx \{(\mathbf{U}^{j+1})^t [\mathbf{U}^j (\mathbf{H}_1^j \mathbf{a}^j)]\}. \tag{B8}$$

We can describe the steps in this equation as follows: one advances the phase of the coefficients to the next segment then one sums up the modes to compute the field just to the left of the interface and finally, one projects the pressure field onto the mode set in the next segment. Computing the coupling matrix would involve the calculation of the matrix–matrix product $(\mathbf{U}^{j+1})^t \mathbf{U}^j$ but when the operations are done in the order indicated by Eq. (B8), one performs only the operation of a matrix times a vector and therefore obtains a significant savings in execution time.

[1] F. D. Tappert, "The parabolic approximation method," in *Wave Propagation in Underwater Acoustics*, edited by J. B. Keller and J. S. Papadakis (Springer-Verlag, New York, 1977), pp. 224–287.

[2] D. Lee, G. Botseas, and J. S. Papadakis, "Finite difference solution of the parabolic equation," J. Acoust. Soc. Am. **70**, 795–800 (1981).

[3] M. D. Collins and E. K. Westwood, "A higher-order energy-conserving parabolic equation for range-dependent ocean depth, sound speed, and density," J. Acoust. Soc. Am. **89**, 1068–1075 (1991).

[4] S. R. Rutherford and K. E. Hawker, "Consistent coupled mode theory of sound propagation for a class of nonseparable problems," J. Acoust. Soc. Am. **70**, 554–564 (1981).

[5] G. A. Kriegsmann, "A multiscale derivation of a new parabolic equation which includes density variations," Comput. Math. Appl. **11**, 817–821 (1985).

[6] D. Lee and S. T. McDaniel, "A finite-difference treatment of interface conditions for the parabolic wave equation: The irregular interface," J. Acoust. Soc. Am. **73**, 1441–1447 (1983).

[7] L. Abrahamsson and H. Kreiss, "Boundary conditions for the parabolic equation in a range-dependent duct," J. Acoust. Soc. Am. **87**, 2438–2441 (1990).

[8] F. B. Jensen and C. M. Ferla, "Numerical solutions of range-dependent benchmark problems in ocean acoustics," J. Acoust. Soc. Am. **87**, 1499–1510 (1990).

[9] R. B. Evans, "A coupled mode solution for acoustic propagation in a waveguide with stepwise depth variations of a penetrable bottom," J. Acoust. Soc. Am. **74**, 188–195 (1983).

[10] E. K. Westwood, "Ray model solutions to the benchmark wedge problems," J. Acoust. Soc. Am. **87**, 1539–1545 (1990).

[11] C. M. Bender and S. A. Orszag, *Advanced Mathematical Methods for Scientists and Engineers* (McGraw-Hill, New York, 1978).

[12] H. Bremmer, "The W. K. B. approximation as the first term of a geometrical-optical series," Comm. Pure Appl. Math. **4**, 105–115 (1951).

[13] L. Nghiem-Phu and F. Tappert, "Modeling of reciprocity in the time domain using the parabolic equation method," J. Acoust. Soc. Am. **78**, 164–171 (1985).